Talanta 81 (2010) 1373–1379

Contents lists available at ScienceDirect

Talanta

journal homepage: www.elsevier.com/locate/talanta

Facile electrocatalytic oxidation of diuron on polymerized nickel hydroxo tetraamino-phthalocyanine modified glassy carbon electrodes

Tawanda Mugadza, Tebello Nyokong*

Chemistry Department, Rhodes University, Grahamstown 6140, South Africa

ARTICLE INFO

Article history:
Received 18 November 2009
Received in revised form 10 February 2010
Accepted 11 February 2010
Available online 18 February 2010

Keywords:
Tetraamino nickel (II) phthalocyanine
Diuron
Cyclic voltammetry
Chronoamperometry

ABSTRACT

The facile electro-oxidation of diuron occurred at a glassy carbon electrode (GCE) modified with polymerized nickel tetraamino-phthalocyanine (NiTAPc), containing O–Ni–O bridges represented as *poly*-Ni(OH)TAPc-GCE. The oxidation of diuron occurred at a potential which is 60 mV less than that of *poly*-NiTAPc (without O–Ni–O bridges) and was accompanied by enhanced catalytic currents. The catalytic rate constant and the diffusion constant were found to be 5.91×10^2 mol^{-1} L s^{-1} and 6.43×10^{-6} cm^2 s^{-1}, respectively. The linear concentration range of diuron was 3.0×10^{-5} to 3.5×10^{-4} mol L^{-1} with a limit of detection (LOD) of 3.3×10^{-7} mol L^{-1} (3δ notation) and a sensitivity of 12.9 A mol^{-1} L cm^{-2}.

1. Introduction

Metallophthalocyanines (MPcs) exhibit a rich electrochemical behaviour due to the accessibility of a range of oxidation states centred on the Pc unit or on the central metal [1]. MPcs are very good electrochemical catalysts and as such they have been used for the detection of many analytes including hydrazine [2,3], pesticides [3–6], dopamine [7] and thiols [3,8]. It has also been reported that electrode fouling observed on bare electrodes can be reduced (or eliminated) using MPc complexes [9,10]. Enhancements in catalytic behaviour and resistance to fouling can be achieved on nickel phthalocyanines following the formation of oxo bridges when continuously cyclised in sodium hydroxide [11,12]. Nickel tetraamino-phthalocyanine (NiTAPc, Fig. 1) and other NiPcs, can be cyclised in 0.1 mol L^{-1} NaOH solution, in an appropriate potential window to activate the O–Ni–O bridges [12], giving *poly*-Ni(OH)Pcs. The O–Ni–O bridges in *poly*-Ni(OH)Pcs show better catalytic properties than *poly*-NiPcs (which does not contain O–Ni–O bridges). *Poly*-Ni(OH)TAPc is highly stable and resistant to surface fouling [9].

The choice of NiTAPc instead of for example nickel tetrasulfophthalocyanine (NiTSPc), whose polymer shows the Ni(III)/Ni(II) process (showing the presence of $Ni(OH)_2$ clusters) without the need for activation as is the case for NiTAPc, where the Ni(III)/Ni(II) process appears only after activation by potential cycling, was based on the fact that the films for NiTAPc were found to be less porous than for NiTSPc [12–14]. This would suggest that when NiTAPc is employed, the bare GCE is not exposed as much as for NiTSPc, hence the choice of NiTAPc in this work.

In this work we report on the electrochemical characterization of diuron, a phenyl-urea pesticide (structure in Scheme 1) on a *poly*-Ni(OH)TAPc modified glassy carbon electrode (GCE), to be referred to as *poly*-Ni(OH)TAPc-GCE. Diuron is a systemic substituted phenyl-urea herbicide, which is easily taken up by the root system of plants and quickly trans-located through the xylem vessels into stems and leaves. Diuron acts by inhibiting the Hill reaction in photosynthesis, thus limiting the production of high energy compounds such as adenosine triphosphate (ATP) which are used for various metabolic processes [15]. Relative to other pesticides of the same type, diuron is considered highly mobile and persistent [16,17]. It is thus important to develop methods that are simple, rapid and reliable for the detection of diuron. Electrochemical methods have been employed for the detection of diuron, however passivation of the electrode surface due to deposition of polymeric products has been observed [18,19]. The oxidation route for diuron is thought to involve the hydrogen ion and an electron, giving rise to a free radical which in turn dimerises (Scheme 1) [20]. The use of phthalocyanines in general and *poly*-Ni(OH)TAPc in particular for electrochemical characterization of diuron has not been explored and is reported in this work for the first time, with the aim of reducing passivation and improving sensitivity.

2. Experimental

2.1. Chemicals and reagents

Sodium acetate and sodium hydroxide were from Saarchem while acetic acid was obtained from Merck, NiTAPc was pre-

* Corresponding author. Tel.: +27 46 6038260; fax: +27 46 6225109.
E-mail address: t.nyokong@ru.ac.za (T. Nyokong).

0039-9140/$ – see front matter © 2010 Elsevier B.V. All rights reserved.
doi:10.1016/j.talanta.2010.02.037

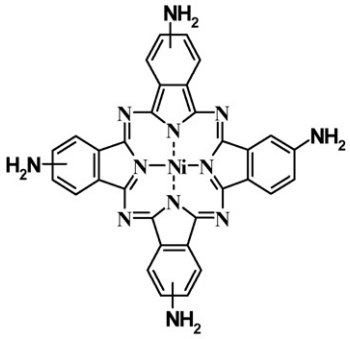

Fig. 1. Structure of nickel tetraamino-phthalocyanine.

pared according to a procedure reported elsewhere [21]. Diuron and tetrabutylammonium tetrafluoroborate ($TBABF_4$) were used as received from Aldrich. Dimethylformamide (DMF) was from Saarchem and was dried and freshly distilled before use. Aqueous solutions were prepared using millipore water from Milli-Q Water Systems (Millipore Corp., Bedford, MA, USA). All other chemicals and reagents were of analytical grade and were used as received. A 1×10^{-3} mol L^{-1} stock solution of diuron was prepared by dissolving the pesticide in methanol and later used to prepare standards using appropriate acetate buffer solutions (pH 3–6).

For the detection of real samples, laboratory tap water and soil from flower beds were employed. The samples were prepared for the analysis as follows: 10 samples (25 g each) of soil and 10 samples (100 mL each) of water were spiked with various known amounts of diuron and left for 5 h. Diuron extracts from the spiked water were recovered through shaking the water sample with two portions of diethyl-ether (50 mL each) in a separating funnel for 10 min and then separating the aqueous phase from the organic phase. Diethyl-ether was then allowed to evaporate slowly overnight in the fume-hood. The residues were dissolved in methanol, transferred to 50 mL volumetric flasks and made up to the mark with pH 4 acetate buffer.

Extracts from the spiked soil samples were recovered through treatment of the sample with 100 mL of acetone and then allowing acetone to evaporate.

2.2. Electrochemical studies

Electrochemical data (cyclic voltammetry and chronoamperometry) was recorded using a Princeton Applied Research potentiostat/galvanostat Model 264. A three component electrochemical cell composed of GCE (area = 0.071 cm^2) as the working electrode, platinum wire (Pt) as a counter electrode and a silver|silver chloride wire (Ag|AgCl) as a pseudo-reference electrode was used. For electro-polymerization, NiTAPc (1×10^{-3} mol L^{-1}) solutions were prepared in DMF using 0.1×10^{-3} mol L^{-1} $TBABF_4$ as a supporting electrolyte. Electro-polymerization, on a glassy carbon electrode (GCE), was performed under continuous potential cycling conditions (cyclic voltammetry) of the solutions of the NiTAPc monomer (1×10^{-3} mol L^{-1}) from −1.0 to +1.3 V (versus Ag|AgCl) at 100 mV/s for 30 cycles, giving *poly*-NiTAPc-GCE.

Before electro-polymerization of NiTAPc, the bare GCE was polished to a mirror finish on a Buehler-felt pad using 0.5 μm alumina paste, and then washed with millipore water, sonicated for 5 min in millipore water, washed again with millipore water and then with the appropriate pH buffer solutions. After each cyclic voltammogram, the modified electrode was rinsed in methanol, then millipore water and cyclised in pH 4 buffer before the next reading was taken.

Poly-NiTAPc-GCE was transformed into *poly*-Ni(OH)TAPc-GCE through repetitive cycling in 0.1 mol L^{-1} NaOH solution in the potential window −1.0 to +1.4 V versus Ag|AgCl at a scan rate of 0.05 V/s for 25 cycles. Prior to the analyses all the solutions were purged with argon gas to drive out oxygen and an atmosphere of argon was maintained throughout the analyses.

The linear dynamic range for diuron has been reported to be between 2.1×10^{-5} to 3.0×10^{-4} mol L^{-1} [22] and 1.2×10^{-5} to 2.5×10^{-4} mol L^{-1} [23] and in this study diuron the linear concentration range was from 3×10^{-5} to 3.5×10^{-4} mol L^{-1}.

3. Results and discussion

3.1. Polymerization of NiTAPc and characterization using cyclic voltammetry

The presence of amino groups on the periphery of the ring results in MPc molecules which can be electro-polymerized onto electrodes. Amino groups are suitable substituents because they

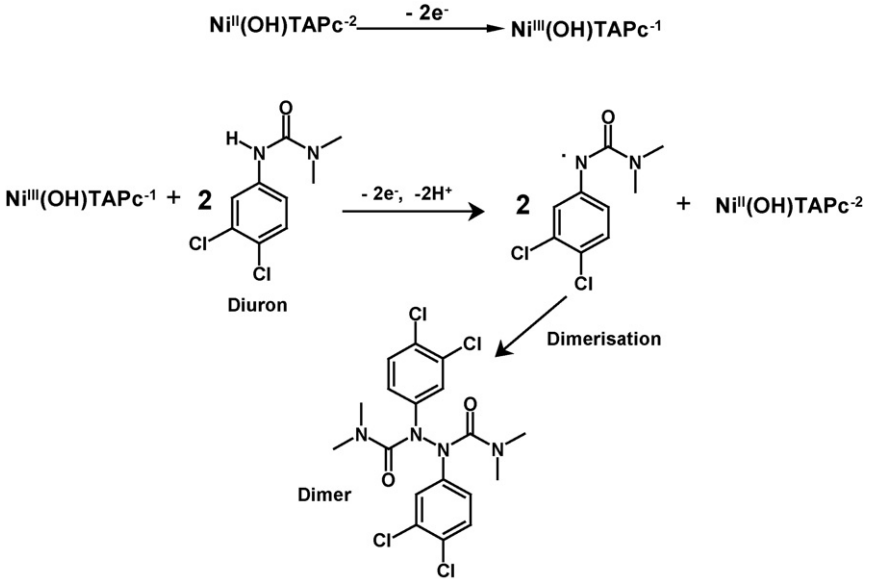

Scheme 1. Mechanism for the electro-catalysis of diuron on *poly*-Ni(OH)TAPc modified electrodes.

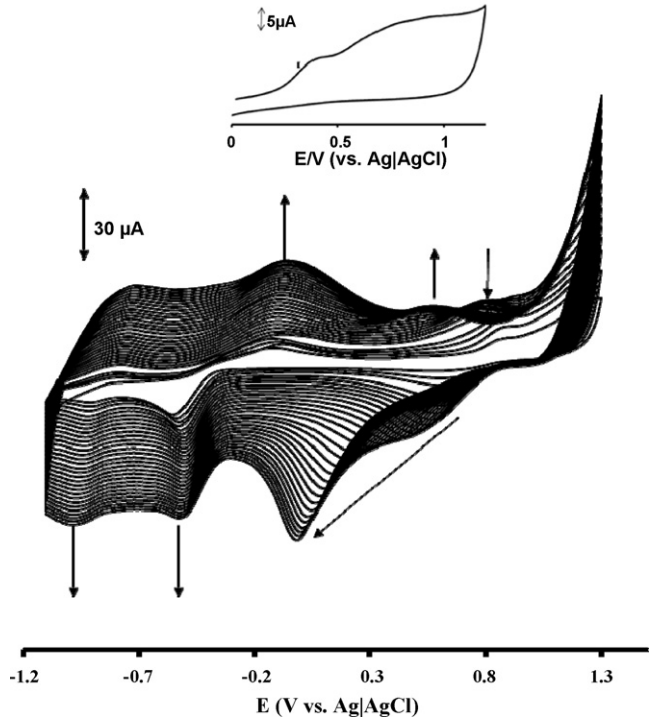

Fig. 2. Repetitive cyclic voltammetry of 1×10^{-3} mol L^{-1} NiTAPc on glassy carbon electrode in DMF containing ~1×10^{-3} mol L^{-1} $TBABF_4$. Inset = the cyclic voltammogram of *poly*-NiTAPc in pH 4 acetate buffer. Scan rate = 100 mV/s.

are able to form a network of conjugated bonds and hence polymerize with ease. Electro-polymerization of NiTAPc complexes is well-established [24,25]. Fig. 2 shows the evolution of cyclic voltammograms during polymerization of NiTAPc monomer in DMF containing $TBABF_4$. The evolution of the polymer in Fig. 2 is similar to that observed in the literature [25], showing well defined redox processes. The inset in Fig. 2 shows the cyclic voltammogram of *poly*-NiTAPc in pH 4 acetate buffer (which is used for diuron detection). The peak labeled I is due to $Ni^{II}Pc^{-1}$ species in accordance with the literature [1].

Poly-NiTAPc (Fig. 2) was transformed into *poly*-Ni(OH)TAPc through repetitive cycling in 0.1 mol L^{-1} NaOH in the potential window −1.0 to +1.4 V versus Ag|AgCl at a scan rate of 0.05 V/s for 25 cycles (Fig. 3a). Fig. 3a (inset) shows expanded view of successive increases in peak currents for the Ni^{III}/Ni^{II} processes (couple II). These processes have been observed in other studies [9,10]. The large increases in currents beyond +0.6 V have been attributed to the electro-oxidation of OH^- ions to O_2 with $OH^\bullet$ radicals as intermediates [10]. Peak I represents the first ring reduction of NiTAPc. Fig. 3b shows the *poly*-Ni(OH)TAPc-GCE in pH 4 buffer with the Ni^{III}/Ni^{II} (process II) being shifted to less positive values compared to NaOH solution in Fig. 3a. Process III in Fig. 3b is due to ring-based process ($Ni^{III}Pc^{-1}$) of adsorbed *poly*-Ni(OH)TAPc.

Fig. 3b (inset) shows the plot of the anodic background corrected peak current versus sweep rate, using process II in Fig. 3b. The linear relationship of the plot of scan rate versus current at these low scan rates is characteristic of surface-immobilized redox species. The surface coverage of the redox active *poly*-Ni(OH)TAPc film was estimated from the plot of background corrected peak current versus scan rate, according to Eq. (1) [26]:

$$I_p = \frac{n^2 F^2 \upsilon A \Gamma_{MPc}}{4RT} \quad (1)$$

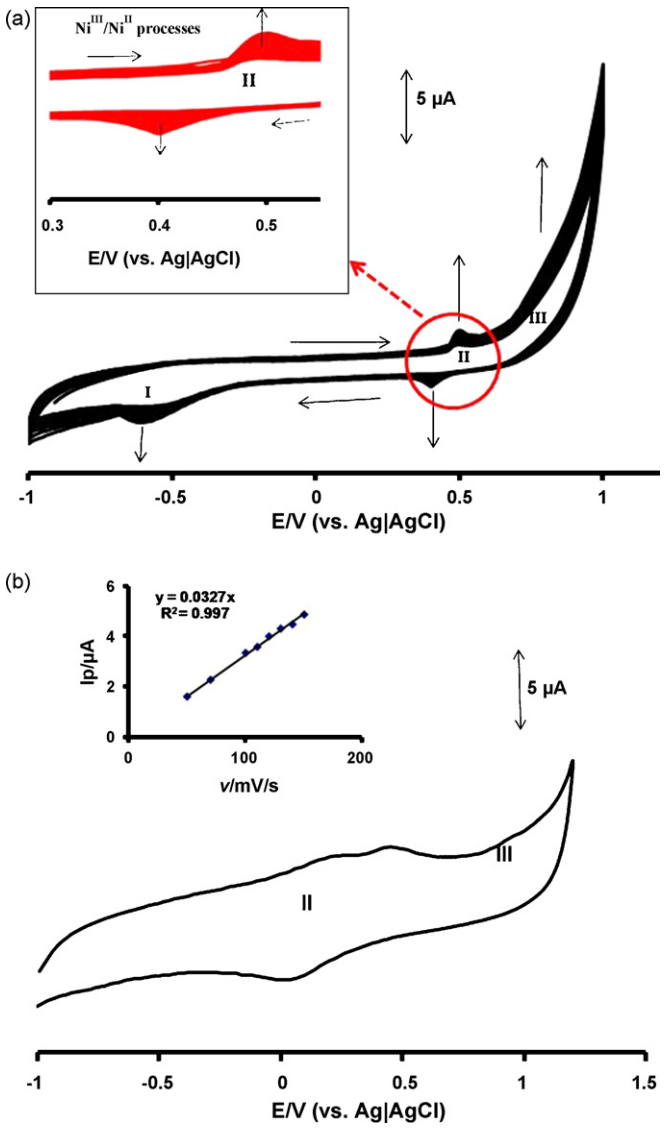

Fig. 3. (a) 25 repetitive scans of *poly*-NiTAPc-GCE in 0.1 mol L^{-1} NaOH (forming *poly*-Ni(OH)TAPc-GCE). Inset: Expanded view showing the Ni(III)/Ni(II) processes. (b) Cyclic voltammogram of *poly*-Ni(OH)TAPc-GCE in pH 4 acetate buffer. Inset: Plot of peak current versus sweep rate for *poly*-Ni(OH)TAPc-GCE in pH 4 acetate buffer. The reduction process of couple II in (b) used. Scan rate = 50 mV/s.

where I_p is the background corrected peak current, n is the number of transferred electrons, F is the Faraday constant, Γ_{MPc} is the film surface coverage, A is the effective electrode area, υ is the scan rate, R is the gas constant and T is the temperature. The Γ_{MPc} value of 1.14×10^{-10} mol cm^{-2} was obtained for *poly*-Ni(OH)TAPc film formed using 25 cycles and using the effective electrode area calculated using Eq. (2) and the cyclic voltammograms of $[Fe(CN)_6]^{4-/3-}$ in 0.1 M of KCl (not shown) [27]:

$$I_{pa} = (2.69 \times 10^5)\, n^{3/2}\, D^{1/2} \upsilon^{1/2} AC \quad (2)$$

where n is the number of electron transferred ($n = 1$), D is the diffusion coefficient of $[Fe(CN)_6]^{3-}$ (7.6×10^{-6} cm^2 s^{-1} [28]), υ is the scan rate, A is the effective surface area, C is the bulk concentration of $[Fe(CN)_6]^{3-}$ (1×10^{-3} mol L^{-1}). The value of $\Gamma_{MPc} = 1.14 \times 10^{-10}$ mol cm^{-2} is in the range for monolayer coverage [21,29,30] for Pc molecule lying flat on the electrode.

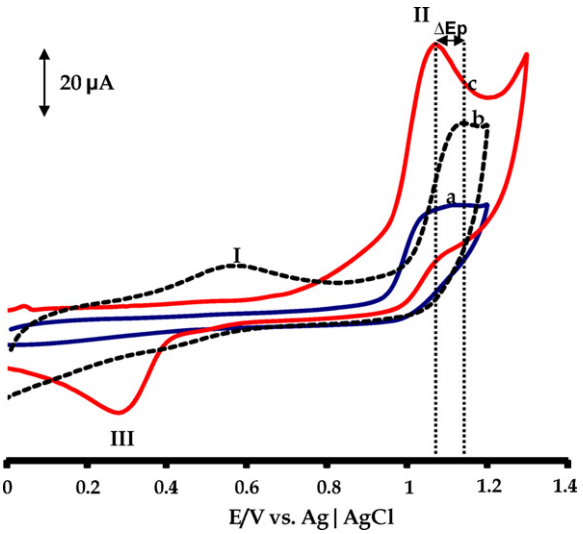

Fig. 4. Cyclic voltammograms of (a) bare GCE, (b) *poly*-NiTAPc-GCE, and (c) *poly*-Ni(OH)TAPc-GCE in 1×10^{-3} mol L^{-1} diuron (pH 4 acetate buffer). Scan rate = 100 mV/s.

3.2. Detection of diuron using cyclic voltammetry

3.2.1. Comparison of poly-Ni(OH)TAPc and poly-NiTAPc

Fig. 4 compares cyclic voltammograms of 1×10^{-3} mol L^{-1} diuron (in pH 4 acetate buffer) on (a) the bare GCE, (b) *poly*-NiTAPc-GCE, and (c) *poly*-Ni(OH)TAPc-GCE. Electro-catalysis is evidenced by a lowering of potential and increase in currents. A large increase in current is observed on *poly*-Ni(OH)TAPc-GCE compared to the bare GCE and the *poly*-NiTAPc-GCE. In turn *poly*-NiTAPc-GCE shows higher currents compared to bare GCE (Fig. 4a). The oxidation potential of diuron on *poly*-Ni(OH)TAPc-GCE occurred at 1.08 V relative to 1.14 V on the *poly*-NiTAPc-GCE, an over-potential difference of 60 mV. The bare GCE had lower currents for diuron detection, but at about the same potential as *poly*-Ni(OH)TAPc (Fig. 4). Thus in terms of catalytic currents the trend for the oxidation of diuron is as follows: *poly*-Ni(OH)TAPc-GCE > *poly*-NiTAPc-GCE > GCE. In terms of potential the order is: *poly*-Ni(OH)TAPc-GCE ~ GCE < *poly*-NiTAPc-GCE. However, the onset of the diuron peak on *poly*-Ni(OH)TAPc-GCE occurs at a lower potential (Fig. 4) compared to GCE and *poly*-NiTAPc-GCE, confirming to effectiveness of the former for diuron oxidation.

Peak I (0.5 V) on the *poly*-NiTAPc-GCE (Fig. 4, see also Fig. 2 inset), is due to redox processes on the Pc ring. Peak III for *poly*-Ni(OH)TAPc is due to Ni^{III} reduction process as observed in other studies [11]. The absence of the anodic peak of the Ni^{III}/Ni^{II} processes on the forward scan suggests that the formed Ni^{III} species is consumed for the oxidation of diuron. The fact that there is a return peak (cathodic) for detection shows that diuron is incapable of reducing the entire Ni^{III} species [31]. Oxidation of diuron (peak II in Fig. 4) occurs at the same potential as the first ring oxidation (process III in Fig. 3b, discussed above), indicating that it is the $Ni^{III}(OH)TAPc^{-1}$ species that are involved in the catalytic oxidation of diuron. For *poly*-NiTAPc-GCE only ring-based processes are involved in catalysis.

3.2.2. pH effects

pH influenced the determination of diuron on GCE and on the modified electrodes. There was a shift in peak potentials to negative values with increase in pH, for process II (in Fig. 4c) as shown in Fig. 5. The slope of the plot in Fig. 5 is 58.6 mV/pH, indicating a transfer of one electron per proton. Scheme 1 represents the proposed one:one electron–proton process [32] leading to the formation of the dimer. In addition, the highest oxidation currents were observed at pH 4 (figure not shown), hence this pH was employed for all studies.

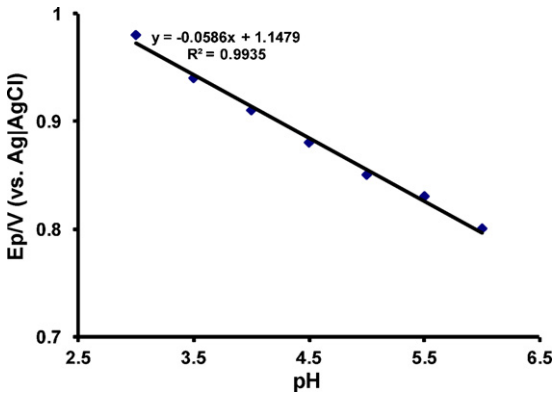

Fig. 5. Plot of peak potential against pH for the detection of 0.1×10^{-3} mol L^{-1} diuron on *poly*-Ni(OH)TAPc-GCE.

3.2.3. Stability

Fig. 6 shows the effect of continuous scanning on the cyclic voltammograms for the detection of diuron (only scans 1, 2, 5 and 15 are shown) on *poly*-Ni(OH)TAPc-GCE. While there is no anodic peak for the Ni^{III}/Ni^{II} couple during the first scan, for the reasons provided above, the anodic peak appears on second scan and increases with scan number and stabilises after cycle 15. The cathodic peak also increases with scan number, but stabilises after scan number 2. The appearance of the Ni^{III}/Ni^{II} process suggests that this process does not catalyse the oxidation of the products obtained on oxidizing diuron. The cathode component is therefore not much affected by continuous scanning, an observation noted by Berríos et al. [12] in their studies with chlorophenols. The decrease in the diuron peak (at 1.08 V) is observed with formation of a new peak at −0.6 V due to the reduction of the oxidation products of diuron. Peak B is due to the oxidation of diuron. The intensity of this peak decreases with the increase in the number of scans, an indication of the passivation of the electrode surface by the diuron oxidation products. There is also an appearance of a new peak, A′ in Fig. 6 which is not present during the first scan. This peak is thus associated with the oxidation of diuron oxidation products formed during the first scan. Peak D is in the region of Ni^{II}/Ni^{I} reduction process and it increases during the first scan, and thereafter decreases. Peak E represents the first ring reduction ($Ni^{I}Pc^{-2}/Ni^{I}Pc^{-3}$) and it increases with the number of scans.

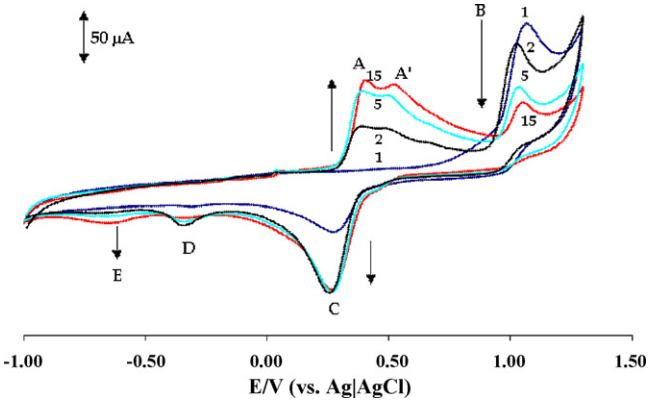

Fig. 6. Cyclic voltammogram cycles 1, 2, 5 and 15 showing the peak behaviour of *poly*-Ni(OH)TAPc-GCE in 1×10^{-3} mol L^{-1} diuron (in pH 4 buffer). Scan rate = 100 mV/s.

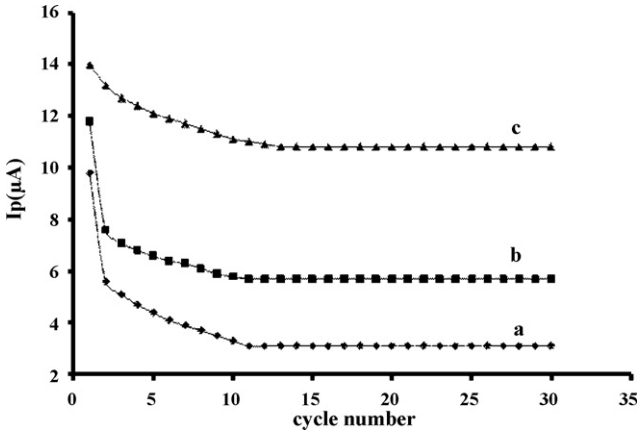

Fig. 7. Plot of the change in peak current, I_p, versus cycle number for (a) bare GCE, (b) *poly*-NiTAPc-GCE and (c) *poly*-Ni(OH)TAPc-GCE in 80 μM diuron in pH 4 buffer. Scan rate = 100 mV/s.

Fig. 7 shows the change in the peak current of diuron with increase in the number of scans. *Poly*-Ni(OH)TAPc-GCE stabilised at 23% of the initial current while *poly*-NiTAPc-GCE and bare GCE stabilised at 52% and 63% of their initial currents, respectively. The drop from the first scan to the second scan was 6%, 36% and 43% for *poly*-Ni(OH)TAPc-GCE, *poly*-NiTAPc-GCE and the bare GCE, respectively, an indication that *poly*-Ni(OH)TAPc-GCE is more resistant to passivation due to the oxidation products. However, the electrode is easily regenerated completely by rinsing in methanol and continuous cyclisation (using cylic voltammetry) in pH 4 acetate buffer. Under continual use, the electrode is stable for up to a period of 3 months if stored in pH 4 acetate buffer.

3.2.4. Kinetics for the catalysis

Fig. 8a shows that the peak potentials increased with scan rate ($\log \upsilon$), thus indicating the chemical irreversibility of the diuron electrocatalytic oxidation process. The Tafel slope for an irreversible diffusion controlled catalytic process was obtained using Eq. (3) [33].

$$E_p = \left(\frac{2.303RT}{2(1-\alpha)}\right) n_\alpha \log \upsilon + K \quad (3)$$

where α is the transfer coefficient, n_α is the number of electrons involved in the rate determining step, υ is the scan rate, K is a constant, T is the temperature and R is the gas constant. From the plot of E_p versus $\log \upsilon$, a Tafel slope of 192 mV/decade was obtained. High Tafel slopes have no kinetic meaning but could indicate a passivation phenomena occurring on the electrode surface. Tafel slopes much greater (>240 mV/decade) than the normal 30–120 mV/decade are known [32,34–36] and have been related either to chemical reactions coupled to electrochemical steps [34] or to substrate–catalyst interactions in a reaction intermediate [32,35,36]. Using the slope of the plot of E_p versus $\log \upsilon$ the value of α was estimated to be 0.71, though this value is not too reliable due to the high Tafel slope.

Fig. 8b also shows a linear relationship between the peak current and square root of the scan rate, indicating that the diuron electrocatalytic oxidation is diffusion controlled. A plot of sweep rate normalised current density ($I_p\, \upsilon^{-1/2}$) versus the sweep rate (Fig. 8c), exhibited a typical shape indicative of a catalytic process with an electrochemical reaction preceding a chemical reaction [37].

3.3. Chronoamperometric studies

Fig. 9a shows single step chronoamperometric evolutions recorded after polarization of the *poly*-Ni(OH)TAPc-GCE in the potential window 0.9–1.2 V in different concentrations of diuron (in pH 4 acetate buffer). Chronoamperometry was used for the determination of the catalytic rate constant at intermediate times (the decreasing part of the curve; t = 0.1–1 s). The catalytic current, I_{cat}, is dominated by the oxidation of diuron. The rate constant (k) for reaction between diuron and redox sites of the surface-immobilized poly-Ni(OH)TAPc is determined according to Eq. (4) [38]:

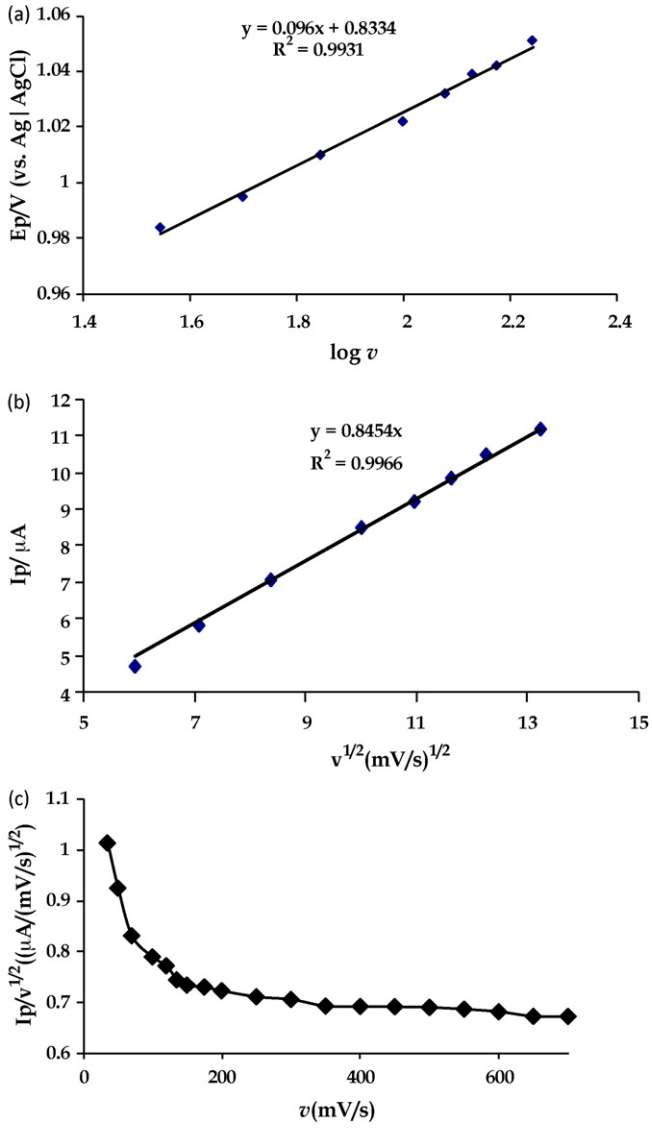

Fig. 8. Plot of (a) peak potential versus $\log \upsilon$, (b) peak current versus square root of sweep rate and (c) sweep rate normalised current versus sweep rate, for 1×10^{-3} mol L^{-1} diuron in pH 4 buffer.

$$\frac{I_{cat}}{I_{buf}} = \gamma^{1/2}\left[\pi^{1/2}\mathrm{erf}(\gamma^{1/2}) + \frac{\exp(-\gamma)}{\gamma^{1/2}}\right] \quad (4)$$

$\gamma = kC_0t$ (C_0 is the bulk concentration of diuron) and $\mathrm{erf}(\gamma^{1/2})$ is the error function. In cases where γ exceeds 2 [38] the error function is almost equal to 1 and Eq. (4) reduces to Eq. (5):

$$\frac{I_{cat}}{I_{buf}} = \gamma^{1/2}\pi^{1/2} = (\pi kC_0t)^{1/2} \quad (5)$$

where I_{cat} and I_{buf} are currents in the presence and absence of diuron, k is the catalytic rate constant (M^{-1} s^{-1}), C_0 is the bulk concentration of diuron (1.4×10^{-4} mol L^{-1}) and t the elapsed time in seconds. From the slope of I_{cat}/I_{buf} versus $t^{1/2}$ plot (Fig. 9b) for 1.4×10^{-4} mol L^{-1} diuron, the value of k was found to

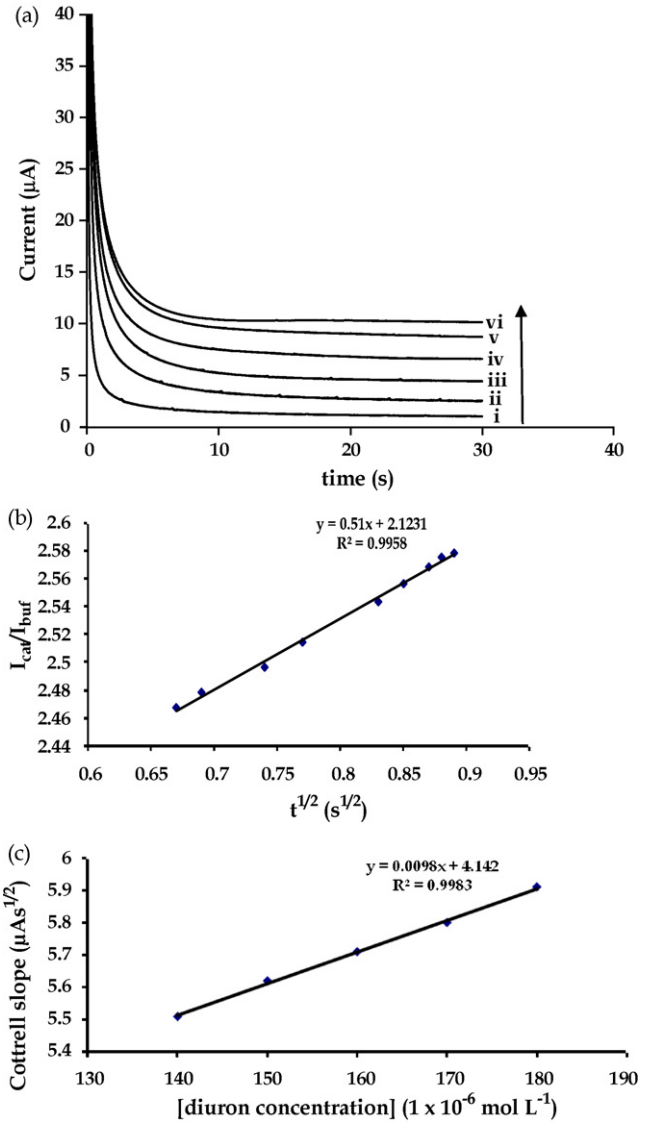

Fig. 9. (a) Chronoamperograms for the various concentrations of diuron in pH 4 acetate buffer on the *poly*-Ni(OH)TAPc-GCE electrode; (i) pH 4 buffer only; diuron concentrations: (ii) 1.4×10^{-4} mol L^{-1}, (iii) 1.5×10^{-4} mol L^{-1}, (iv) 1.6×10^{-4} mol L^{-1}, (v) 1.7×10^{-4} mol L^{-1} and (vi) 1.8×10^{-4} mol L^{-1}. (b) Plot of I_{cat}/I_{buf} versus $t^{1/2}$ for the catalytic oxidation diuron *poly*-Ni(OH)TAPc-GCE; (c) Cottrell slopes versus diuron concentrations. Potential = 1.2 V.

be 5.91×10^2 mol^{-1} L s^{-1}. Unfortunately no information could be obtained from the literature on the catalytic rate constants for the electrochemical oxidation of diuron or other phenyl-ureas.

The diffusion coefficient, *D*, for diuron was determined from Eq. (6) [38]:

$$I = nFD^{1/2}AC_0\pi^{-1/2}t^{-1/2} \quad (6)$$

where *C* is the bulk concentration of diuron, *F* is the Faraday's constant, *A* is the electrode area, *n* is the number of electrons, and *t* is the time in seconds.

From the slopes of Cottrell plots (*I* versus $t^{-1/2}$) for different concentrations of diuron, Fig. 9c was obtained, giving an estimated value of *D* of 6.43×10^{-6} cm^2 s^{-1}. Again no information could be obtained from the literature on the catalytic rate constants for the electrochemical oxidation of diuron or other related compounds.

A linear equation of plot of current versus the concentration of diuron obtained using chronoamperometry was obtained with a correlation coefficient of 0.9974. A sensitivity of 12.9 A mol^{-1} L cm^{-2} (r^2 = 0.9974) and a detection limit (LOD) of 3.3×10^{-7} mol L^{-1} using the 3δ/slope ratio notation (where δ is the standard deviation of the plot) were obtained. The response due to the blank (buffer alone) constitutes the background current. On addition of diuron to the buffer, the current responses were at levels above that of the background. After comparing the current responses in the absence and presence of diuron at a particular time (at *t* = 5 s in this study), the concentration of diuron was calculated. Using this method, very low levels of diuron, close to the LOD were obtained. This would imply that the operational limit of detection could be similar to the LOD obtained through the 3δ criterion. A LOD of 6.59×10^{-6} mol L^{-1} has been reported for diuron using capillary electrophoresis and electrochemical detection [22]. A LOD of 4.7×10^{-6} and 4.0×10^{-6} mol L^{-1} has been observed for diuron using capillary electrophoresis coupled with UV and electrochemical detectors, respectively [23]. Thus, this method gives a favorable LOD compared to the literature, hence confirming the sensitivity of *poly*-Ni(OH)TAPc-GCE towards the detection of diuron.

3.4. Analysis of environmental samples

The suitability of the developed electrode for electrochemical detection of diuron was done in real samples by confirming known concentrations of the herbicide in tap water and in agricultural soil according to the procedure outlined in the experimental section. Overall average recoveries of 99 ± 0.1% of the spikes were observed for the water and soil samples. This demonstrated the suitability of the developed method. The repeatability expressed as the relative standard deviation (RSD) was ±0.102% tap water and ±0.105% for soil for the 10 samples. The obtained data show the accuracy and precision of the developed method. The electrode showed the same stability as was observed above for the standard diuron and the electrode could be renewed similarly.

4. Conclusion

The O–Ni–O bridged *poly*-Ni(OH)TAPc-GCE showed excellent electrocatalytic activity and robust stability and highly resistant to passivation. The electrode is easily regenerated by continuous cyclisation in pH 4 acetate buffer. Very low LODs were obtained relative to other established methods. High diuron recoveries observed are an indication of the suitability and reliability of the proposed method of analysis. Chronoamperometry was used in the determination of the catalytic rate constant and the diffusion coefficient.

Acknowledgements

This work was supported by the Department of Science and Technology (DST) and National Research Foundation (NRF) of South Africa through DST/NRF South African Research Chairs Initiative for Professor of Medicinal Chemistry and Nanotechnology and Rhodes University. TM thanks NRF/DST/D. E. Goddards for the scholarship.

References

[1] A.B.P. Lever, E.R. Milaeva, G. Speier, in: C.C. Leznoff, A.B.P. Lever (Eds.), Phthalocyanines: Properties and Applications, vol. 3, VCH Publishers, New York, 1993, p. 1.
[2] D.A. Geraldo, C.A. Togo, J. Limson, T. Nyokong, Electrochim. Acta 53 (2008) 8051.
[3] T. Nyokong, in: J.H. Zagal, F. Bedioui, J.-P. Dodelet (Eds.), N_4-Macrocyclic Metal Complexes, Springer, New York, 2006.
[4] M.P. Siswana, K.I. Ozoemena, T. Nyokong, Electrochim. Acta 52 (2006) 114.
[5] M. Sbai, H. Essis-Tome, U. Gombert, T. Breton, M. Pontie, Sens. Actuators B: Chem. B124 (2007) 368.
[6] I. Tapsoba, S. Bourhis, T. Feng, M. Pontie, Electroanalysis 21 (2009) 1167.
[7] A. Goux, F. Bedioui, L. Robbiola, M. Pontie, Electroanalysis 15 (2003) 969.
[8] J. Pillay, K.I. Ozoemena, Electrochim. Acta 52 (2007) 3630.
[9] J. Obirai, F. Bedioui, T. Nyokong, J. Electroanal. Chem. 576 (2005) 323.

[10] M.S. Ureta-Zanartu, P. Bustos, M.C. Diez, M.L. Mora, C. Gutierrez, Electrochim. Acta 46 (2001) 2545.
[11] B.O. Agboola, K.I. Ozoemena, T. Nyokong, Electrochim. Acta 51 (2006) 6470.
[12] C. Berríos, J.F. Marco, C. Gutiérrez, M.S. Ureta-Zañartu, Electrochim. Acta 54 (2009) 6417.
[13] M.S. Ureta-Zañartu, C. Berríos, J. Pavez, J. Zagal, C. Gutíerrez, J.F. Marco, J. Electroanal. Chem. 553 (2003) 147.
[14] C. Berríos, M.S. Ureta-Zañartu, C. Gutíerrez, Electrochim. Acta 53 (2007) 792.
[15] Environmental Monitoring Branch, Department of Pesticide Regulation (DPR) California, Pesticide Chemistry Database, 2003.
[16] L. Guzzella, E. Capri, A. Di Corcia, A. Barra Carracciolo, G. Giuliano, J. Environ. Qual. 35 (2006) 312.
[17] K. Abass, P. Reponen, M. Turpeinen, J. Jalonen, O. Pelkonen, Am. Soc. Pharm. Exp. Tech. 35 (2007) 1634.
[18] A.M. Polcaro, M. Mascia, S. Palmas, A. Vacca, Electrochim. Acta 49 (2004) 649.
[19] D. De Souza, R.A. de Toledo, A. Galli, G.R. Salazar- Banda, M.R.C. Silva, G.S. Garbellini, L.H. Mazo, L.A. Avaca, S.A.S. Machado, Anal. Bioanal. Chem. 387 (2007) 2245.
[20] K. Macounova, J. Klima, C. Bernard, C. Degrand, J. Electroanal. Chem. 457 (1998) 141.
[21] M.P. Somashekarappa, J. Keshavayya, S. Sampath, Pure Appl. Chem. 74 (2002) 1609.
[22] M. Chicharro, E. Bermejo, A. Sanchez, A. Zapardiel, A. Fernandez-Gutierrez, D. Arraez, Anal. Bioanal. Chem. 382 (2005) 519.
[23] M. Chicharro, A. Zapardiel, E. Bermejo, A. Sanchez, R. Gonzalez, Electroanalysis 16 (2004) 312.
[24] Z.-H. Wen, T.-F. Kang, Talanta 62 (2004) 351.
[25] J.-P. Fan, X.-M. Zhang, M. Ying, J. Solid State Electrochem. 12 (2008) 1143.
[26] D. Martel, N. Sojic, A. Kuhn, J. Chem. Educ. 79 (2002) 349.
[27] H.O. Finklea, in: A.J. Bard, I. Rubinstein (Eds.), Electroanalytical Chemistry, vol. 19, Marcel Dekker, New York, 1996.
[28] J.J. Gooding, V.G. Praig, E.A.H. Hall, Anal. Chem. 70 (1998) 2396.
[29] S. Griveau, V. Albin, T. Pauporteĭ, J.H. Zagal, F. Bedioui, J. Mater. Chem. 12 (2002) 225.
[30] Z. Li, M. Lieberman, W. Hill, Langmuir 17 (2001) 4887.
[31] S. Majdi, A. Jabbari, H. Heli, A.A. Moosavi-Movahedi, Electrochim. Acta 52 (2007) 4622.
[32] B. Wermeckes, F. Beck, Electrochim. Acta 30 (1985) 1491.
[33] A.J. Bard, L.R. Faulkner, Electrochemical Methods, Fundamentals and Applications, Wiley, New York, 1980.
[34] C.A. Caro, F. Bedioui, J.H. Zagal, Electrochim. Acta 47 (2002) 1489.
[35] M.E.G. Lyons, C.A. Fitzgerald, M.R. Smyth, Analyst 119 (1994) 855.
[36] J.-M. Zen, A. Senthil Kumar, M.-R. Chang, Electrochim. Acta 45 (2000) 1691.
[37] S.M. Golabi, H.R. Zare, J. Electroanal. Chem. 465 (1999) 168.
[38] M.H. Pournaghi-Azar, R. Sabzi, J. Electroanal. Chem. 543 (2003) 115.